International Journal of Automotive Technology, Vol. 24, No. 1, pp. 23–33 (2023)
DOI 10.1007/s12239–023–0003–z

pISSN 1229–9138/ eISSN 1976–3832

PARALLEL PARKING PATH PLANNING BASED ON IMPROVED ARCTANGENT FUNCTION OPTIMIZATION

Qiping Chen[1)*], Lu Gan[1)], Bo Chen[1)], Qin Liu[2)] and Xiaobo Zhang[2)]

[1)]Key Laboratory of Conveyance and Equipment Ministry of Education, East China Jiaotong University, Nanchang 330013, China
[2)]Jiangling Motor Co., Ltd., No. 2111, Yingbin Middle Avenue, Nanchang County, Nanchang City, Jiangxi Province, Nanchang 330001, China

(Received 26 April 2022; Revised 11 June 2022; Accepted 15 June 2022)

ABSTRACT–Aiming at the problems of small parking space and poor parking effect for existing parallel parking, this paper proposes a parallel parking path planning based on improved arctangent function optimization. Firstly, the vehicle parking kinematics model is established, and the vehicle parameters are determined according to the three classical models. Secondly, the parking space model is established, and the most reasonable parking space parameters are selected according to the minimum parking space. Then, aiming at the problems of abrupt curvature of the designed arc-line-arc initial path, unsmooth path, large yaw angle at the end and large parking space, an improved arctangent function model is proposed, the parking constraints are established, the absolute value of vehicle yaw angle is taken as the objective function, and the parameters are optimized by genetic algorithm. Finally, it is verified by simulation experiments. The results show that the method can achieve smoother path, smaller parking space and more ideal parking posture, meet the requirements of stability, safety and comfort in the process of parallel parking, and improve the ability of parallel parking. Therefore, this method can provide a theoretical reference for path planning in automatic parking technology.

KEY WORDS : Parallel parking, Path planning, Improved arctangent function, Parking constraints, Genetic algorithm

1. INTRODUCTION

With the continuous increase of vehicle ownership, it not only brings convenient transportation, but also brings more problems, and especially the problem of difficult parking is becoming more and more serious (Tang *et al*., 2019). The shortage of urban land resources leads to narrow parking spaces, which brings inconvenience to parking and frequent parking accidents. How to improve the handling of vehicles in the parking environment, eliminate potential collision hazards, and park vehicles in the parking space safely and smoothly has gradually attracted people's attention (Dreyfuss *et al*., 2022). Automatic parking technology can not only effectively solve the problem of difficult parking in narrow parking spaces, reduce the occurrence of parking collision accidents and improve the safety in the process of parking, but also alleviate the tension of drivers when parking, reduce the difficulty of parking and improve the comfort of driving (Ma *et al*., 2017; Li *et al*., 2020). As an important part of automatic parking technology, in-depth study of path planning is of great significance to solve the parking problem.

**Corresponding author*. e-mail: 2758@ecjtu.edu.cn

In recent years, researchers are constantly improving the parking path from all aspects. Han (2021) studied a path planning method based on ant colony optimization and grid method. Firstly, the grid method is used to model the parking environment, simulate the actual parking space of automatic parking, then search for an optimal broken line path based on ant colony algorithm, and finally smooth the path through Bessel curve. Cai *et al.* (2022) proposed are planning method based on geometric planning. Compared with other path planning methods, this method performs well in terms of maneuver times and planning time. Huang *et al*. (2022) proposed a cubic polynomial method based on scattering points and transition curve for parking path planning to solve the problem of unsmooth path curve of arc-line combination and sudden change at the junction. Aiming at the problem of abrupt change of path curvature in traditional double arc parking path planning, Li *et al*. (2021) proposed an improved double arc parking trajectory fitting method to meet the requirements of parking path curvature and steering angular velocity. Yu *et al*. (2021) proposed a new method of training Bezier curve control points using radial basis function neural network method in order to optimize the continuous curvature, safety and meeting curvature constraints of the initial planned path of vehicles during parallel parking. This method effectively

improves the ability of parallel parking of small vehicles. In order to develop an automatic parking system, Li *et al*. (2020) innovatively proposed a preview correction algorithm that can be used for parking path planning. Through this algorithm, the curvature outliers in the parking path are detected, so as to obtain a fast, safe and stable parking path. However, the algorithm is complex and has poor real-time performance. Jiang *et al*. (2017) in order to solve the problem of curvature discontinuity in the path planning of traditional circular arc straight line combination curve, the path is smoothed by quintic polynomial. The optimized path has good continuity, which makes the whole parking process smoother, but has great requirements for parking space. Lee *et al*. (2020) proposed a robust parking path planning method with error adaptive sampling to solve the problem that vehicles cannot park safely to the correct position under the condition of perceived uncertainty. This method makes the generated adaptive path continuously consider the detection error, and has the advantages of strong adaptability and high precision, but the path curvature fluctuates obviously and does not perform well in comfort.

In view of the problems of small parking space and poor parking effect faced by the existing parallel parking, based on the arc-line-arc combined path, this paper proposes a parallel parking path planning based on improved arctangent function optimization, and has made three contributions:

(1) This paper can effectively solve the problem of discontinuous mutation of the curvature of the arc-line-arc path curve at the connection, and can generate a continuous, safe and smooth parking path for the three classic models, with high safety, strong comfort and good robustness.
(2) The genetic algorithm is used to optimize the parameters to find an optimal path, so as to occupy fewer parking spaces and meet the requirements of smaller parking space.
(3) This paper can effectively solve the problem that the vehicle is not parallel to the parking space and the parking posture is poor, which makes the yaw angle at the parking end 0 and make the posture more ideal.

In this paper, firstly, the vehicle parking kinematics model is established, and the vehicle parameters are determined according to the three classical models. At the same time, the parking space model is established, and the most reasonable parking space parameters are selected according to the minimum parking space. Secondly, in order to make the planning path simple and effective, an initial path scheme of arc-line-arc is designed. Then, aiming at the problems of abrupt curvature change in the initial path, unsmooth path, large yaw angle at the end and large parking space, an improved arctangent function model is proposed, and the parking constraints are established. Then, the ideal goal is to minimize the absolute value of yaw Angle at the terminal point, the absolute value of yaw angle is regarded as the objective function, and the genetic algorithm is used to optimize the parameters. Finally, it is verified by simulation experiments.

2. MODEL ESTABLISHMENT AND PARAMETER SELECTION

2.1. Establishment of Vehicle Parking Kinematics Model

In the process of parking, the vehicle speed is mostly within 6 km/h, and the side slip phenomenon is negligible (Chen *et al*., 2017). The whole body can be regarded as a rigid body, so the vehicle kinematics model is established, which is shown in Figure 1.

Here, θ is the vehicle yaw angle; φ is the equivalent angle of steering wheel; Points A, B, C and D are the four vertices of the vehicle contour; r is the center point of the rear axle; f is the center point of the front axle; W_r is the rear track width; W is the vehicle width; l is the wheelbase; l_f is front suspension; l_r is the rear suspension.

The coordinates of the center point r of the rear axle of the vehicle are recorded as (x_r, y_r), and the coordinates of the four vertices A, B, C and D of the vehicle can be obtained as follows:

$$\begin{cases} x_A = x_r + (l + l_f)\cos\theta - \dfrac{W\sin\theta}{2} \\ y_A = y_r + (l + l_f)\sin\theta + \dfrac{W\cos\theta}{2} \end{cases} \tag{1}$$

$$\begin{cases} x_B = x_r - l_r\cos\theta - \dfrac{W\sin\theta}{2} \\ y_B = y_r - l_r\sin\theta + \dfrac{W\cos\theta}{2} \end{cases} \tag{2}$$

$$\begin{cases} x_C = x_r - l_r\cos\theta + \dfrac{W\sin\theta}{2} \\ y_C = y_r - l_r\sin\theta - \dfrac{W\cos\theta}{2} \end{cases} \tag{3}$$

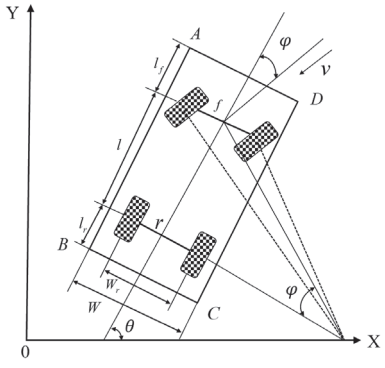

Figure 1. Vehicle parking kinematics model.

$$\begin{cases} x_D = x_r + (l + l_f)\cos\theta + \dfrac{W\sin\theta}{2} \\ y_D = y_r + (l + l_f)\sin\theta - \dfrac{W\cos\theta}{2} \end{cases} \tag{4}$$

In addition, the motion trajectory equations of the four vertices A, B, C and D of the parking system are:

$$\begin{cases} x_A(t) = (l\cot\varphi - \dfrac{W}{2})\sin\theta + (l + l_f)\cos\theta \\ y_A(t) = -(l\cot\varphi - \dfrac{W}{2})\cos\theta + (l + l_f)\sin\theta + l\cot\varphi \end{cases} \tag{5}$$

$$\begin{cases} x_B(t) = (l\cot\varphi - \dfrac{W}{2})\sin\theta - l_r\cos\theta \\ y_B(t) = -(l\cot\varphi - \dfrac{W}{2})\cos\theta - l_r\sin\theta + l\cot\varphi \end{cases} \tag{6}$$

$$\begin{cases} x_C(t) = (l\cot\varphi + \dfrac{W}{2})\sin\theta - l_r\cos\theta \\ y_C(t) = -(l\cot\varphi - \dfrac{W}{2})\cos\theta - l_r\sin\theta + l\cot\varphi \end{cases} \tag{7}$$

$$\begin{cases} x_D(t) = (l\cot\varphi + \dfrac{W}{2})\sin\theta + (l + l_f)\cos\theta \\ y_D(t) = -(l\cot\varphi + \dfrac{W}{2})\cos\theta + (l + l_f)\sin\theta + l\cot\varphi \end{cases} \tag{8}$$

2.2. Establishment of Parking Space Model

Parking is mainly divided into vertical parking, oblique parking and parallel parking (Jing *et al*., 2021). Compared with vertical parking and oblique parking, parallel parking is more complex, the parking space is narrow, and parking is more difficult. Therefore, this paper mainly takes parallel parking as the research object, and establishes the schematic diagram of parking space model as shown in Figure 2. Here, D is the road width; L_r is the length of parking space; W_r is the width of the parking space and *a*, *b*, *c*, *d* is the four vertices of the parking space.

2.3. Selection of Vehicle Parameters

According to the actual parking investigation, this paper selects three classic models for parallel parking research. The parameters of the three classic models are shown in Table 1.

Here, L is the train length; W is the vehicle width; l is the wheelbase; l_f is front suspension; l_r is rear suspension; W_f is the front track width; W_r is the rear track width; $R_{\min}$ is the minimum turning radius.

2.4. Selection of Parking Space Parameters

Theoretically, the larger the parking space, the less difficult it is to park, and the higher the parking controllability, but the corresponding problem of parking space tension caused by the large parking space area is highlighted. Therefore, in order to determine the parking space with the minimum limit, a schematic diagram of the minimum parking space is established as shown in Figure 3.

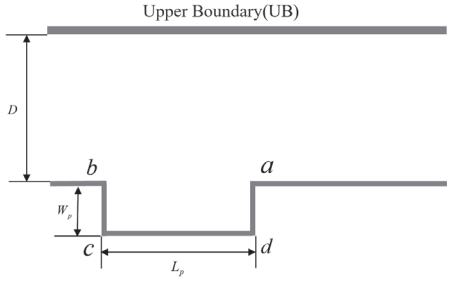

Figure 2. Schematic diagram of parking space mode.

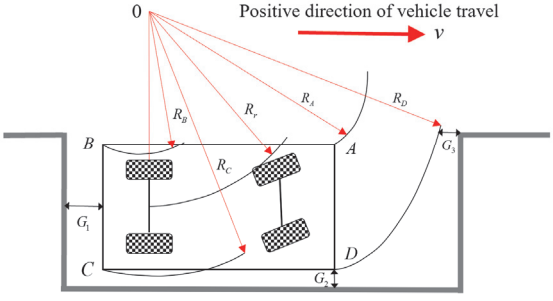

Figure 3. Schematic diagram of minimum parking space.

Table 1. Parameters of three classic models.

Vehicle model	Vehicle parameters (m)						
	L	W	l	l_f	l_r	W_f	W_r
Mini vehicle	2.920	1.493	1.940	0.540	0.440	1.290	1.290
Ordinary vehicle	4.980	1.910	2.920	1.020	1.040	1.530	1.530
SUV	4.645	1.860	2.680	0.951	1.014	1.580	1.580

Here, R_A, R_B, R_C, R_D, R_r is the circular motion radius of the four vertices of the vehicle body and the center of the rear axle of the vehicle respectively, and G_1, G_2, G_3 is the safe space maintained by the left boundary, lower boundary and right boundary of the vehicle body and the parking space respectively.

From the geometric relationship shown in Figure 3, the relationship of R_C, R_D can be obtained as follows:

$$R_C = \sqrt{(R_r + \frac{W}{2})^2 + l_f^2} \tag{9}$$

$$R_D = \sqrt{(R_r + \frac{W}{2})^2 + (l + l_f)^2} \tag{10}$$

Combined with Figure 1 and Table 1, the parking space meets the following constraints:

$$\begin{cases} L_p \geq \sqrt{R_D^2 - (R_r - \frac{W}{2})^2} + G_1 + G_3 \\ W_p \geq \frac{W}{2} + (R_C - R_r) + G_2 \end{cases} \tag{11}$$

Substitute (9) into formula (10):

$$\begin{cases} L_{p\_min} = \sqrt{(R_r + \frac{W}{2})^2 + (l + l_f)^2} - (R_r - \frac{W}{2})^2 + G_1 + G_3 \\ W_{p\_min} = \frac{W}{2} + (\sqrt{(R_r + \frac{W}{2})^2 + l_f^2} - R_r) + G_2 \end{cases} \tag{12}$$

Here, the value of G_1, G_2, G_3 is 0.1m according to literature (Zhang *et al.*, 2022). Therefore, according to formula (12) and the vehicle parameters in Table 1, the relationship curve between vehicle turning radius and parking space length and width is established as shown in Figure 4.

Figure 4 shows that the length of parking space is directly proportional to the turning radius of vehicle, and the width of parking space is inversely proportional to the turning radius of vehicle. With the increasing turning radius of vehicles, the length of the minimum parking space changes more than the width. According to the structural characteristics of the vehicle, the turning radius of the vehicle must be greater than or equal to the minimum turning radius of the vehicle during parking. Therefore, the length of the parking space is taken as the selection standard of the size of the parking space. By substituting

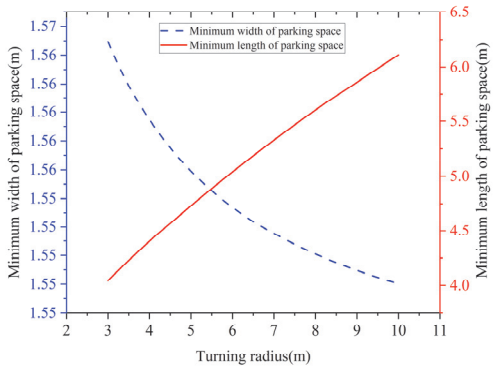

(a) Mini vehicle

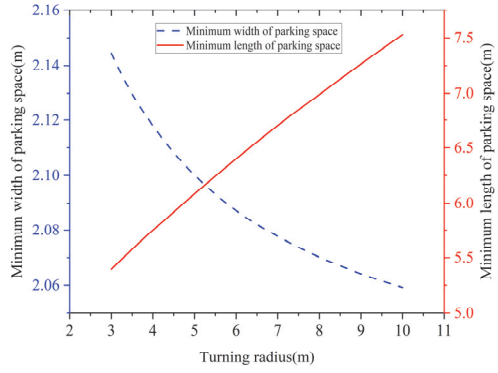

(b) Ordinary vehicle

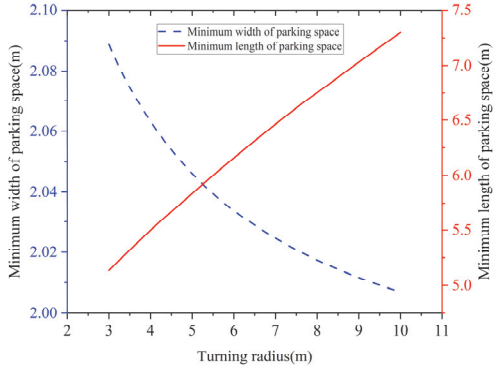

(c) SUV

Figure 4. Relationship curve between turning radius of vehicle and length and width of parking space.

the structural parameters of the three vehicles into formula (12), the minimum parking space can be obtained as follows: 4.40 × 1.56 m, 6.15 × 2.10 m, 6.00 × 2.04 m. According to *Garage building design code JGJ100-2015* (Beijing Jianzhu University, 2015), the limit minimum standard parking space parameter finally selected in this paper is 6.4 × 2.4 m, and the road width D is 4 m.

3. PARALLEL PARKING INITIAL PATH PLANNING

Planning a reasonable reference path can not only avoid the collision between the vehicle and the surrounding obstacles during parking, but also park the vehicle to the designated position and occupy a small parking space. Therefore, based on the advantages of simple calculation of arc-arc combined path planning (Kim *et al*., 2010), this paper designs an arc-line-arc combined parallel parking path planning scheme, as shown in Figure 5.

Here, *e*, *f*, *g*, *h* is the boundary point of arc, straight line and arc respectively; d_1 is the distance between the vehicle body and the parking space on the side close to the parking space at the beginning of parking; d_2 is the absolute value of the abscissa change of the center of the rear axle of the vehicle during the whole parking process; d_3 is the absolute value of the longitudinal coordinate change of the center of the rear axle of the vehicle during the whole parking process; D is the width of the road; α is the angle of the circular arc section of the vehicle. R_1, R_2 is the radius of two arcs.

The whole parking can be simply divided into three stages: arc *ef*, line *fg*, arc *gh*. The first stage is that the vehicle travels from position *e* to position *f* along the first arc; The second stage is that the vehicle travels from position *f* to position *g* along a straight line; The third stage is that the vehicle travels from position *g* to position *h* along the second arc.

According to the geometric relationship and vehicle structural parameters shown in Figure 5, the following can be obtained:

$$\begin{cases} R_2 \cdot \sin\alpha + l_{fg} \cdot \cos\alpha + R_1 \sin\alpha = d_2 \\ (R_2 - R_1\cos\alpha) + l_{fg} \cdot \sin\alpha + (R_1 - R_1\cos\alpha) = d_3 \end{cases} \tag{13}$$

The motion trajectory equations of the center of the rear axle of the vehicle in the three stages of arc *ef*, straight line *fg* and arc *gh* are respectively:

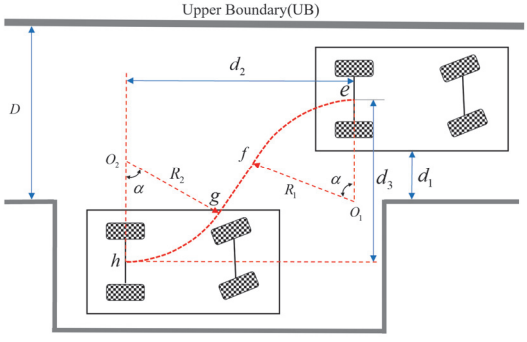

Figure 5. Arc-line-arc combined parallel parking path planning scheme.

$$(x - d_2)^2 + (y + (R_1 - d_3))^2 = R_1^2 \tag{14}$$

$$kx + y + a = 0 \tag{15}$$

$$x^2 + (y - R_2)^2 = R_1^2 \tag{16}$$

In order to shorten the length of the parking path, the minimum turning radius $R_{\min}$ is used for the radius of the motion of the two arcs. It can be seen that $R_1 = R_2 = R_{\min}$, and the corresponding center coordinates are: $O_1(d_2, R_{\min} - d_3)$, $O_2(0, R_{\min})$.

Assuming that the distance between the centers of two circles and straight line *fg* is l_{O_1f}, l_{O_2g}, $l_{O_1f} = l_{O_2g} = R_{\min}$ can be obtained. According to the geometric relationship, the lengths of l_{O_1f} and l_{O_2g} are respectively:

$$\begin{cases} l_{O_1f} = \dfrac{\left|k \cdot d_2 + (R_{\min} - d_3) + a\right|}{\sqrt{k^2 + 1}} \\ l_{O_2g} = \dfrac{\left|R_{\min} + a\right|}{\sqrt{k^2 + 1}} \end{cases} \tag{17}$$

According to $l_{O_1f} = l_{O_2g} = R_{\min}$, the slope k and variable parameter a of segment l_{fg} can be solved:

$$\begin{cases} k = \dfrac{(d_3 - 2R_{\min}) \cdot d_2 + \sqrt{(1 - d_2^2 + 4R_{\min}) \cdot d_3^2 + 4R_{\min}(d_2 - 1 - R_{\min}^2) \cdot d_3 + 4R_{\min}^2}}{d_2^2 - 4R_{\min}^2} \\ a = R\min(1 - \sqrt{1 + k^2}) \end{cases} \tag{18}$$

It is easy to know that the rotation angle α is the arctangent of the slope k, from which we can get:

$$\alpha = \arctan k \tag{19}$$

The length of segment l_{fg} is:

$$l_{fg} = \frac{d_2 - 2R_{\min}\sin\alpha}{\cos\alpha} \tag{20}$$

4. IMPROVED ARCTANGENT FUNCTION OPTIMIZATION PATH

4.1. Improved Design of Arctangent Function

According to the similarity between arc-line-arc combined path trajectory and arctangent function and the nonlinear characteristics of parking trajectory, an improved arctangent function model is proposed to optimize the path. The optimization function model is as follows:

$$y = a_1 \arctan(a_2 x^3 + a_3 x^2 + a_4 x + a_5) + a_6 \tag{21}$$

Here, x, y is the coordinate of vehicle parking path; a_1, a_2, a_3, a_4, a_5, a_6 is an unknown constant.

Substituting the coordinates of the starting point $e(x_e, y_e)$ into the formula (21):

$$a_6 = y_e - a_1 \arctan(a_2 x_e^3 + a_3 x_e^2 + a_4 x_e + a_5) \tag{22}$$

The derivation of formula (22) shows that:

$$\dot{y}_e = \frac{a_1(3a_2 x_e^2 + 2a_3 x_e + a_4)}{1 + (a_2 x_e^3 + a_3 x_e^2 + a_4 x_e + a_5)^2} \tag{23}$$

Assuming that the vehicle body is parallel to the coordinate X axis at the parking starting point e, the numerator in formula (23) is 0, which can be obtained as follows:

$$a_4 = -(3a_2 x_e^2 + 2a_3 x_e) \tag{24}$$

4.2. Establishment of Parking Constraints

Parking constraints include environmental collision constraints, vehicle full seating constraints, vehicle parallel to parking space constraints and maximum radius of curvature constraints. In order to facilitate the description of parking constraint space, a rectangular coordinate system is established with the vertex b of parking space as the coordinate origin, and the schematic diagram of parking constraint analysis is constructed as shown in Figure 6.

4.2.1. Environmental collision constraints

In the parking environment, in order to ensure no collision with surrounding obstacles during parking, environmental collision constraints are established. The schematic diagram of environmental collision is shown in Figure 7, and the constraints are as follows:

In order to avoid collision with the boundary on the road (UB), the left front vertex A of the vehicle body shall be higher than the road width D, and the constraints satisfied are:

$$y_A < D + W_p, x \in [0, x_e] \tag{25}$$

The contour line on the right side of the vehicle shall avoid collision with the top angle a of the parking space. The right body shall be higher than the vertex of parking space a, and the constraints satisfied are:

$$\tan\alpha(L_p - x_a) + y_a \geq W_p, x_B \geq L_p \cap x_C \leq L_p \tag{26}$$

In order to avoid collision with the parking space boundary, vertex D on the right side of the vehicle meets the following constraints:

$$x_D \leq L_p, y_D > 0 \tag{27}$$

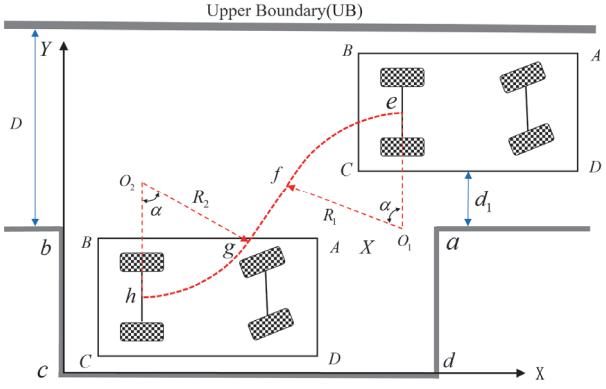

Figure 6. Schematic diagram of parking constraint analysis.

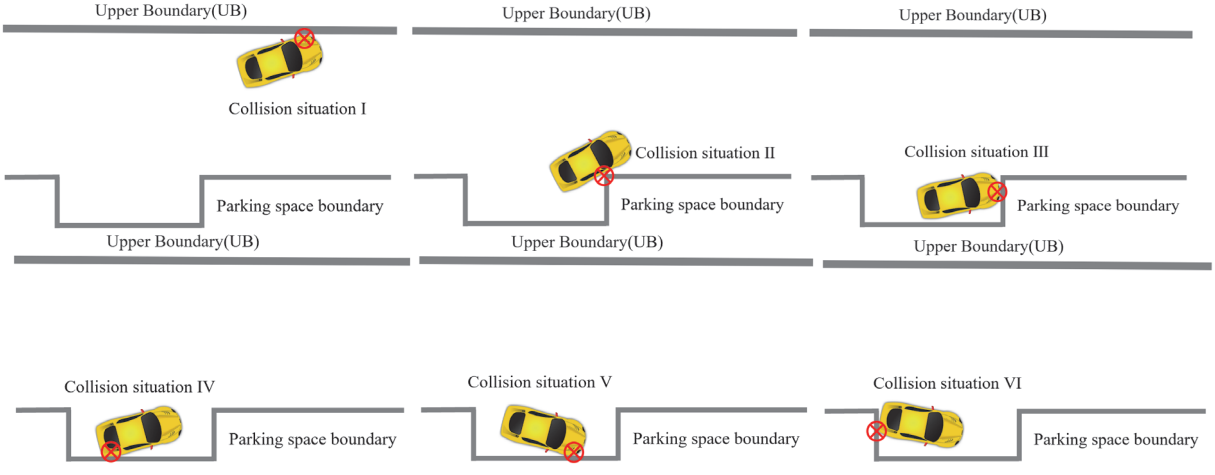

Figure 7. Schematic diagram of environmental collision.

After the vehicle is parked in the parking space, avoid the lower part of the vehicle body from touching the parking space boundary, and the constraints met are:

$$\begin{cases} y_C > 0, x \in [0, L_p] \\ y_D > 0, x \in [0, L_p] \end{cases} \tag{28}$$

After the vehicle is parked in the parking space, the rear of the vehicle body shall not touch the parking space boundary, and the constraints met are:

$$\begin{cases} x_B \geq 0, x \in [0, x_e] \\ x_C \geq 0, x \in [0, x_e] \end{cases} \tag{29}$$

4.2.2. Vehicle fully seated constraint

In order to make the vehicle fully park in the parking space during parking, the vehicle full seating constraint is established as shown in Figure 8. Therefore, it is required that the two vertices A and B on the vehicle body shall not be higher than the upper boundary of the parking space, and the constraints satisfied are:

$$y_A \leq W_p, y_B \leq W_p, x \in [0, L_p] \tag{30}$$

4.2.3. Vehicle parallel to parking space constraint

In order to make the starting point and end point of parking parallel to the parking space, the constraints satisfied are:

$$\begin{cases} \theta = \dfrac{180}{\pi} \cdot \arctan[a_1 \arctan(a_2 x^3 + a_3 x^2 \\ \qquad + a_4 x + a_5) + a_6], x \in [x_e, x_h] \\ \theta \leq \Delta, x = x_e, x = x_h \end{cases} \tag{31}$$

In order to simplify the calculation and reduce the parking path error, try to keep the vehicle coincident with the starting point of the desired path at the starting point of parking, so as to meet the following constraints:

$$\left\| (x_e - x_q) + (y_e - y_q) \right\| \leq \Delta \tag{32}$$

Here, (x_q, y_q) is the starting point of the path and Δ is the error value. According to relevant literature (Li *et al*., 2013), Δ is taken as 0.001.

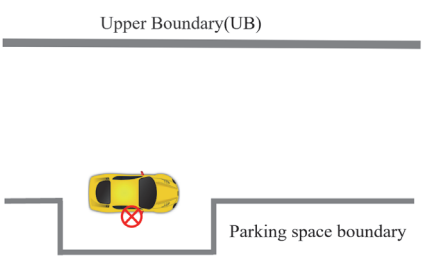

Figure 8. Schematic diagram of vehicle not fully entering the parking space.

4.2.4. Radius constraint of maximum curvature

In order to ensure that the radius of curvature required in the path is less than the allowable maximum curvature value that the vehicle can achieve, the radius constraint of maximum curvature is established, that is, the maximum value $|K|$ of path curvature cannot exceed the allowable maximum turning radius K_{max}, and the constraints satisfied are:

$$\begin{cases} K = \dfrac{|\dot{x}\ddot{y} - \ddot{x}\dot{y}|}{(\dot{x}^2 + \dot{y}^2)^{\frac{3}{2}}} \\ K_{\max} = \dfrac{1}{R_{\min}} \\ |K| \leq K_{\max} \end{cases} \tag{33}$$

To sum up, the parking space constraints to be met in the whole parking process are divided into equality constraints and inequality constraints. The equality constraints are shown in formula (34) and the inequality constraints are shown in formula (35).

$$\begin{cases} x_A = x_r + (l + l_f) \cdot \cos\theta - \dfrac{W \cdot \sin\theta}{2} \\ y_A = y_r + (l + l_f) \cdot \sin\theta + \dfrac{W \cdot \cos\theta}{2} \\ x_B = x_r - l_r \cdot \cos\theta - \dfrac{W \cdot \sin\theta}{2} \\ y_B = y_r - l_r \cdot \sin\theta + \dfrac{W \cdot \cos\theta}{2} \\ x_C = x_r - l_r \cdot \cos\theta + \dfrac{W \cdot \sin\theta}{2} \\ y_C = y_r - l_r \cdot \sin\theta - \dfrac{W \cdot \cos\theta}{2} \\ x_D = x_r + (l + l_f) \cdot \cos\theta + \dfrac{W \cdot \sin\theta}{2} \\ y_D = y_r + (l + l_f) \cdot \sin\theta - \dfrac{W \cdot \cos\theta}{2} \\ \theta = \dfrac{180}{\pi} \cdot \arctan[a_1 \arctan(a_2 x^3 + a_3 x^2 \\ \qquad + a_4 x + a_5) + a_6], x \in [x_e, x_h] \\ K = \dfrac{|\dot{x}\ddot{y} - \ddot{x}\dot{y}|}{(\dot{x}^2 + \dot{y}^2)^{\frac{3}{2}}} \\ K_{\max} = \dfrac{1}{R_{\min}} \\ a_6 = y_e - a_1 \arctan(a_2 x_e^3 + a_3 x_e^2 + a_4 x_e + a_5) \\ a_4 = -(3a_2 x_e^2 + 2a_3 x_e) \end{cases} \tag{34}$$

$$\begin{cases} y_A < D + W_p, x \in [0, x_e] \\ \tan\alpha(L_p - x_a) + y_a \geq W_p, \\ \quad x_B \geq L_p, x_C \leq L_p \\ x_D \leq L_p, y_D > 0 \\ y_C > 0, x \in [0, L_p] \\ y_D > 0, x \in [0, L_p] \\ x_B \geq 0, x \in [0, x_e] \\ x_C \geq 0, x \in [0, x_e] \\ y_A \leq W_p, y_B \leq W_p, x \in [0, L_p] \\ \theta \leq \Delta, x = x_e, x = x_h \\ \left\|(x_e - x_q) + (y_e - y_q)\right\| \leq \Delta \\ \left|K\right| \leq K_{\max} \end{cases} \tag{35}$$

4.3. Genetic Algorithm Optimization

Genetic algorithm will find a set of parameters that not only meet the constraints, but also make the objective function reach the minimum and optimal. It is expected that the smaller the absolute value of yaw angle θ after parking, the better. Therefore, the paper takes yaw angle θ as the objective function of genetic algorithm.

The premise of using genetic algorithm is to solve the problems of initial population setting, coding mode, selection operator, crossover operator, mutation operator, evaluation function and termination standard. In this paper, MATLAB 2021a software is used to plan the path by calling the ga function in the genetic algorithm toolbox. The steps are as follows:

(1) Call the ga function in the genetic algorithm toolbox and initialize to obtain the initial value randomly generated by array N:

$$A_i = (a_1, a_2, a_3, a_5), i = 1, 2, 3, \cdots, N \tag{36}$$

(2) Substitute the starting point $e(x_e, y_e)$ and formula (36) into formula (22) and (24), and calculate:

$$A_i = (a_4, a_6), i = 1, 2, 3, \cdots, N \tag{37}$$

(3) Integrate formulas (36) and (37), and define the fitness function as:

$$\begin{aligned} &finesfcn(A_i) = \left|y_e - y_h\right| \\ &+ \left|\arctan(\dot{y}_e \times \pi / 180)\right|, i = 1, 2, 3, \cdots, N \end{aligned} \tag{38}$$

(4) If the constraints of formulas (34) and (35) cannot be satisfied, the fitness function returns an infinite value:

$$\begin{aligned} &finesfcn\left[A_i = (a_1, a_2, a_3, a_4, a_5, a_6)\right] \\ &= \inf, i = 1, 2, 3, \cdots, N \end{aligned} \tag{39}$$

(5) If the termination condition of ga function is satisfied, go to step (6), otherwise go to the next generation calculation according to genetic algorithm and go to step (2);

(6) The genetic algorithm terminates and obtains the optimal parameters $A_i = (a_1, a_2, a_3, a_4, a_5, a_6)$.

5. SIMULATION ANALYSIS

According to the selected three classic vehicle parameters and parking space parameters, based on the initial planning path of arc-line-arc, the control point $A_i = (a_1, a_2, a_3, a_4, a_5, a_6)$ is solved through the improved arctangent function model. Taking the absolute value of yaw angle θ as the objective function, the control point $A_i = (a_1, a_2, a_3, a_4, a_5, a_6)$ is optimized through genetic algorithm, and the following simulation is obtained. In the Tables 2 ~ 4, $|K|_{\max}$ is the maximum radius of curvature of the path; $K_{\max}$ is the maximum curvature radius allowed by the vehicle; θ_h is the curvature value at the parking end of the vehicle; R is the ratio of parking space length to vehicle length.

5.1. Simulation Scheme 1: Mini Vehicle (2.92 × 1.493 m)

In Figure 9 (a), due to the large ratio of parking space length to vehicle length (R = 2.19178), sufficient parking space and large adjustable space, there is no contact and collision with the environment during the whole parking process, and the vehicle is fully seated, meeting the requirements of environmental collision constraints and vehicle fully seated constraints. In Figure 9 (b), the transition of path curvature line is smooth and there is no sudden change, which indicates that the parking process is continuous, and the vehicle runs smoothly and comfortably. In Table 2, the maximum radius of curvature $|K|_{\max}$ of the optimized path trajectory curvature is 0.225868, which is less than the maximum radius of curvature $K_{\max}$ 0.25 allowed by the vehicle, meeting the radius constraint requirements of the maximum curvature; The yaw angle θ_h at the end of parking approaches 0, which indicates that the vehicle body is parallel at the end of parking and meets the requirements of vehicle parallel to parking space constraint.

5.2. Simulation Scheme 2: Ordinary Vehicle (4.98 × 1.91 m)

In Figure 10 (a), although the ratio of parking space length to vehicle length (R = 1.2851) is small, the parking space is compact, and the adjustable space is small, when the vehicle enters the parking space, there is no contact and collision with the environment during the whole parking process, and the vehicle is fully seated, meeting the requirements of environmental collision constraints and vehicle fully seated constraint. In Figure 10 (b), the transition of the curvature line of the path track is smooth without sudden change, which indicates that the parking process is continuous, the vehicle runs smoothly and has

Table 2. Simulation results of mini vehicle.

Mini vehicle			
(x_e, y_e)	(7.2876,3.7437)	a_1	1.429
(x_h, y_h)	(0.51,1.31)	a_2	-0.01522
$\|K\|_{max}$	0.225868	a_3	0.1858
K_{max}	0.25	a_4	0.1067
θ_h	0	a_5	-1.57
R	2.19178	a_6	2.626

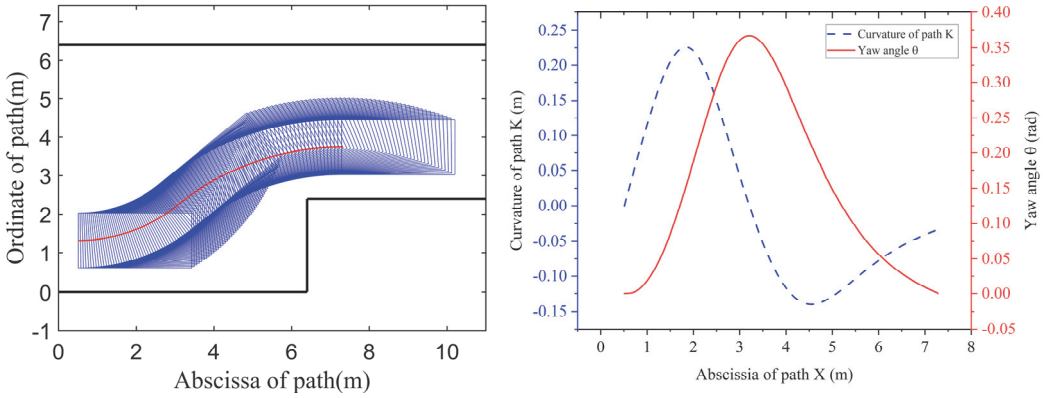

(a) Parking path trajectory (b) Curvature and yaw angle diagram

Figure 9. Simulation diagram of mini vehicle.

Table 3. Simulation results of ordinary vehicle.

Ordinary vehicle			
(x_e, y_e)	(7.1634, 3.7336)	a_1	-0.8987
(x_h, y_h)	(0.32, 1.22)	a_2	-0.1466
$\|K\|_{max}$	0.185693	a_3	1.365
K_{max}	0.1923	a_4	-4.854
θ_h	0	a_5	5.918
R	1.2851	a_6	2.395

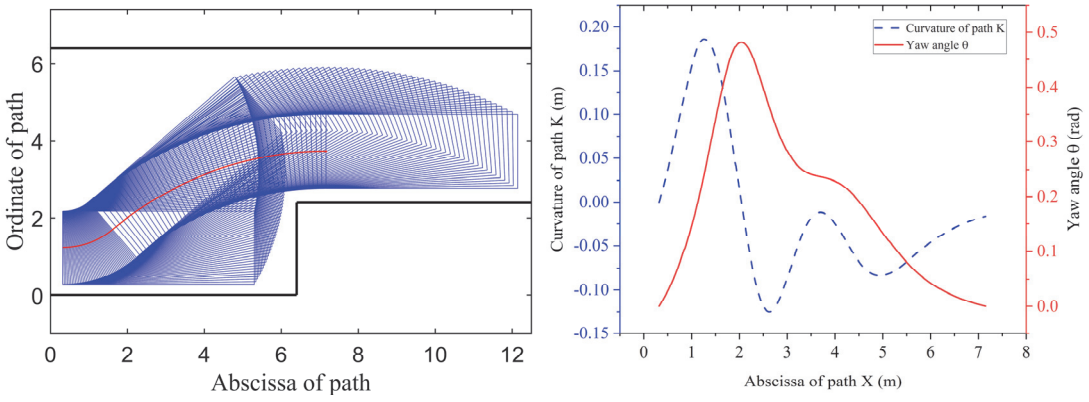

(a) Parking path trajectory (b) Curvature and yaw angle diagram

Figure 10. Simulation diagram of ordinary vehicle.

Table 4. Simulation results of SUV.

SUV			
(x_e, y_e)	(7.3393,3.864)	a_1	0.9179
(x_h, y_h)	(0.48,1.25)	a_2	0.1511
$\|K\|_{max}$	0.179111	a_3	-1.602
K_{max}	0.181818	a_4	6.344
θ_h	0	a_5	-8.713
R	1.3778	a_6	2.512

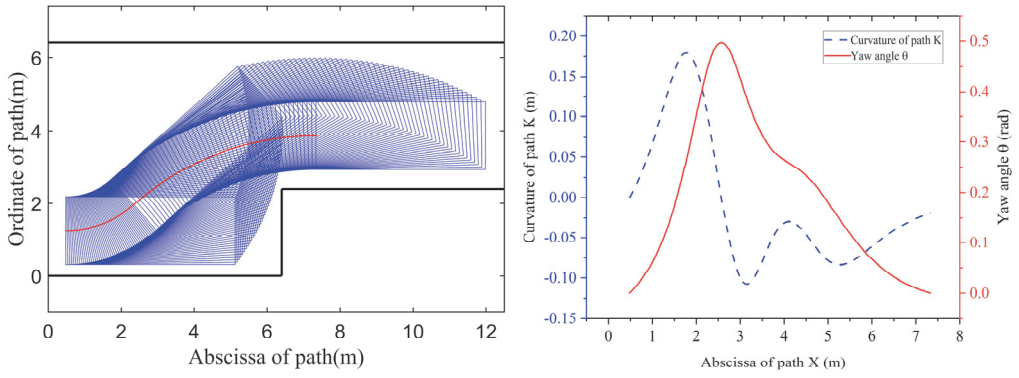

(a) Parking path trajectory

(b) Curvature and yaw angle diagram

Figure 11. Simulation diagram of SUV.

good comfort. In Table 3, the maximum radius of curvature $|K|_{max}$ of the optimized path trajectory curvature is 0.185693, which is less than the maximum radius of curvature K_{max} 0.1923 allowed by the vehicle, meeting the radius constraint requirements of the maximum curvature; The yaw angle θ_h at the end of parking approaches 0, which indicates that the vehicle body is parallel at the end of parking and meets the requirements of vehicle parallel to parking space constraint.

5.3. Simulation Scheme 3: SUV (4.645 × 1.86 m)

In Figure 11 (a), although the ratio of parking space length to vehicle length (R = 1.3778) is small, the parking space is compact, and the adjustable space is small, when the vehicle enters the parking space, there is no contact and collision with the environment during the whole parking process, and the vehicle is fully seated, meeting the requirements of environmental collision constraints and vehicle fully seated constraint. In Figure 11 (b), the transition of the curvature line of the path trajectory is smooth without sudden change, which indicates that the parking process is continuous, the vehicle runs smoothly and has good comfort. In Table 4, the maximum radius of curvature $|K|_{max}$ of the optimized path trajectory curvature is 0.179111, which is less than the maximum radius of curvature K_{max} 0.181818 allowed by the vehicle, meeting the radius constraint requirements of the maximum curvature; The yaw angle θ_h at the end of parking approaches 0, which indicates that the vehicle body is parallel at the end of parking and meets the requirements of vehicle parallel to parking space constraint.

Table 5. Ratio of parking space length to vehicle length.

This paper	Zhang *et al.* (2022)	Lin *et al.* (2012)	Wang *et al.* (2011)
1.2851	1.30	1.35	1.38

The above simulation schemes show that different types of vehicles can realize safe, continuous and stable parking, and verify the effectiveness, safety, comfort and robustness of this method. In addition, as shown in Table 5, the parallel parking path planning method proposed in this paper obtains a smaller ratio of parking space length to vehicle length (R = 1.2851), which is reduced by 1.146 %, 4.807 % and 6.876 % respectively.

6. CONCLUSION

Firstly, this paper establishes the vehicle kinematics model, selects the vehicle reference parameters of common models, establishes the parking space model, and selects the reasonable parking space parameters according to the

calculated minimum parking space. Secondly, in order to make the planned path simple and effective, a parallel parking initial path of arc-line-arc is planned according to the vehicle kinematics model and parking space model. Then, aiming at the problems of abrupt curvature and uneven path in the initial path of parallel parking, an improved arctangent function model is proposed, and the parking constraint space is established. The ideal goal is to minimize the absolute value of yaw Angle at the terminal point, the absolute value of yaw angle is regarded as the objective function, and the genetic algorithm is used to optimize the parameters. Finally, through the simulation experiment, a smooth and no mutation parallel parking path curve is obtained. The minimum ratio of parking space to vehicle length is 1.2851, the required parking space is smaller, the yaw angle at the parking end is close to 0, and the parking posture is more ideal. The proposed method can not only realize the accurate parking of three classic models, but also has strong robustness. It can make the optimized path smoother and easier to control, meet the requirements of stability, safety and comfort in the process of parallel parking, and improve the ability of parallel parking.

In the future, corresponding research will be carried out on other parking situations such as vertical parking spaces and oblique parking spaces.

ACKNOWLEDGEMENT–This research was supported by the National Natural Science Foundation of China (Grant No. 52162044), the Key Research Program of Jiangxi Province (Grant No. 20212BBE51014), the Nanchang Key Laboratory of Intelligent and Connected New Energy Vehicles (Grant No. 2020-NCZDSY-006), and the High-end Talents Project of Science and Technology Innovation of Jiangxi Province (Grant No. JXSQ 2019201119).

REFERENCES

Beijing Jianzhu University (2015). *Garage Building Design Code JGJ100-2015*. China Architecture and Building Press. Beijing, China.

Cai, L., Guan, H., Zhang, H. L., Jia, X. and Zhan, J. (2022). Multi-maneuver vertical parking path planning and control in a narrow space. *Robotics and Autonomous Systems*, **149**, 103964.

Chen, W., Fang, Y. and Wei, Z. (2017). Path planning of two-direction vertical parking based on optimization with genetic algorithm. *Qiche Gongcheng/Automotive Engineering* **39**, **11**, 1325–1332.

Dreyfuss, M., Shaki, Y. Y. and Yechiali, U. (2022). The double-space parking problem. *OR Spectrum*, 1–17.

Han, G. L. (2021). Automatic parking path planning based on ant colony optimization and the grid method. *J. Sensors*, **2021**, 8592558.

Huang, J., Yang, Y., Ding, D., Li, Y. and He, Y. (2022). Automatic parking paths planning research based on scattering points six-degree polynomial and easement curve. *Proc. Institution of Mechanical Engineers, Part D: J. Automobile Engineering*, 09544070221076594.

Jiang, H. B., Shen, Z. N., Shidian, M. A. and Chen, L. (2017). Intelligent identification of automatic parking system based on information fusion. *J. Mechanical Engineering* **53**, **22**,125–133.

Jiang, W., Xin, X., Chen, W. and Cui, W. (2021) Multi-condition parking space recognition based on information fusion and decision planning of automatic parking system. *J. Mechanical Engineering* **57**, **6**, 131–141.

Kim, D., Chung, W. and Park, S. (2010). Practical motion planning for car-parking control in narrow environment. *IET Control Theory & Applications* **4**, **1**, 129–139.

Lee, S., Lim, W. and Sunwoo, M. (2020). Robust parking path planning with error-adaptive sampling under perception uncertainty. *Sensors* **20**, **12**, 3560.

Li, C., Jiang, H., Ma, S., Jiang, S. and Li, Y. (2020). Automatic parking path planning and tracking control research for intelligent vehicles. *Applied Sciences* **10**, **24**, 9100.

Li, H., Guo, K. H., Song, X. L. and Li, F. (2013). Trajectory planning of automatic parallel parking with multi-constraints based on Matlab. *J. Central South University (Science and Technology)* **44**, **1**, 102.

Li, M., Zhou, P., He, X., Lv, H. and Zhang, H. (2021). Parallel parking path planning and tracking control based on adaptive algorithms. *Int. J. Automotive Technology* **22**, **4**, 949–965.

Lin, Z. Z., Li, Q., Liang, Y. J. and Cheng, D. (2012). Parallel parking algorithm based on autonomous path planning. *Application Research of Computers* **29**, **5**, 1713–1715.

Ma, S., Jiang, H., Han, M., Xie, J. and Li, C. (2017). Research on automatic parking systems based on parking scene recognition. *IEEE Access*, **5**, 21901–21917.

Tang, C., Yang, J., Wang, K. and Dalian, M. (2019). Concept of elevated city and three layer model for urban space. *Chinese J. Underground Space and Engineering* **15**, **3**, 637–642.w

Wang, D., Liang, H., Mei, T. and Zhu, H. (2011). Research on self-parking path planning algorithms. *IEEE Int. Conf. Vehicular Electronics and Safety (ICVES)*, Beijing, China.

Yu, L., Wang, X., Hou, Z., Du, Z., Zeng, Y. and Mu, Z. (2021). Path planning optimization for driverless vehicle in parallel parking integrating radial basis function neural network. *Applied Sciences* **11**, **17**, 8178.

Zhang, B., Li, Z., Ni, Y. and Li, Y. (2022). Research on path planning and tracking control of automatic parking system. *World Electric Vehicle J.*, **13**, **1**, 14.